



Photochemical Efficiency of Photosystem II in Inverted Leaves of Soybean [*Glycine max* (L.) Merr.] Affected by Elevated Temperature and High Light

Cong Wang¹, Qiuli Gu², Lianjia Zhao³, Chunyan Li², Jintao Ren¹ and Jianxin Zhang^{1*}

¹ College of Agriculture, Xinjiang Agricultural University, Urumqi, China, ² Agriculture and Rural Bureau of Qapqal County, Qapqal County, China, ³ Research Institute of Crop Germplasm Resources, Xinjiang Academy of Agricultural Sciences, Urumqi, China

OPEN ACCESS

Edited by:

Fabrizio Eulalio Leite Carvalho,
Corporacion Colombiana
de Investigacion Agropecuaria
(Agrosavia) – CI La Suiza, Colombia

Reviewed by:

Sajad Hussain,
Sichuan Agricultural University, China
Marian Brestic,
Slovak University of Agriculture,
Slovakia

*Correspondence:

Jianxin Zhang
onion2021@126.com

Specialty section:

This article was submitted to
Crop and Product Physiology,
a section of the journal
Frontiers in Plant Science

Received: 22 September 2021

Accepted: 07 December 2021

Published: 16 February 2022

Citation:

Wang C, Gu Q, Zhao L, Li C,
Ren J and Zhang J (2022)
Photochemical Efficiency
of Photosystem II in Inverted Leaves
of Soybean [*Glycine max* (L.) Merr.]
Affected by Elevated Temperature
and High Light.
Front. Plant Sci. 12:772644.
doi: 10.3389/fpls.2021.772644

In summer, high light and elevated temperature are the most common abiotic stresses. The frequent occurrence of monsoon exposes the abaxial surface of soybean [*Glycine max* (L.) Merr.] leaves to direct solar radiation, resulting in irreversible damage to plant photosynthesis. In this study, chlorophyll a fluorescence was used to evaluate the functional status of photosystem II (PSII) in inverted leaves under elevated temperature and high light. In two consecutive growing seasons, we tested the fluorescence and gas exchange parameters of soybean leaves for 10 days and 15 days (5 days after recovery). Inverted leaves had lower tolerance compared to normal leaves and exhibited lower photosynthetic performance, quantum yield, and electron transport efficiency under combined elevated temperature and high light stress, along with a significant increase in absorption flux per reaction center (RC) and the energy dissipation of the RC, resulting in significantly lower performance indexes (PI_{ABS} and PI_{total}) and net photosynthetic rate (P_n) in inverted leaves. High light and elevated temperature caused irreversible membrane damage in inverted leaves, as photosynthetic performance parameters (P_n , PI_{ABS} , and PI_{total}) did not return to control levels after inverted leaves recovered. In conclusion, inverted leaves exhibited lower photosynthetic performance and PSII activity under elevated temperature and high light stress compared to normal leaves.

Keywords: high light, elevated temperature, leaf inversion, photosynthesis, chlorophyll a fluorescence

INTRODUCTION

Soybean leaves are heterogeneous, and the adaxial surface is the major contributor to carbon gain because the adaxial surface palisade tissue is rich in chloroplasts and exposed to direct radiation (Evans, 1999). However, some plant leaves are inverted or wobbly due to cultivation conditions (e.g., water and fertilizer) and wind (Zhang et al., 2016; Paradiso et al., 2020). Due to the difference in anatomy between the abaxial and adaxial surfaces of soybeans, their response to environmental conditions can vary, especially light conditions (Hughes and Smith, 2007). Therefore, studying the

response of inverted leaves to the environment will provide a theoretical basis for exploring ways to minimize damage to the photosynthetic apparatus.

Soybean is one of the most important oil crops in the world (Cai et al., 2020); due to human factors and frequent natural disasters, the global average temperature will continue to rise rapidly in the future; and unfavorable high temperatures will affect plant growth and development (IPCC, 2019), usually causing reversible/irreversible damage to different organs of the plant, this is because leaf photosynthesis is one of the most sensitive processes to elevated temperatures in plants (Yamori and Shikanai, 2016; Mihaljević et al., 2020). Under natural conditions, the elevated temperatures at noon in summer are usually accompanied by other environmental stresses, such as high light, and the dual stress of heat and high light seriously affects the growth and development of soybeans, especially during the seed-filling stage, resulting in reduced soybean yields (Cohen et al., 2021; Kimm et al., 2021). As an important organ in direct contact with the environment, leaves are more sensitive to light and temperature, because photosystem II (PSII) is sensitive to heat and high irradiation stress during the process of carbon dioxide assimilation (Dongsansuk et al., 2013; Jiang et al., 2021). Exposure to high light and elevated temperature in summer can damage the photosynthetic apparatus of the plant and cause photoinhibition, which is manifested in the metabolic processes: reduced transpiration accompanied by increased leaf temperature, reduced antioxidant and photosynthetic enzyme activities, damage to the cytoplasmic membrane, destruction of chloroplast structure and function, reduced electron transport and carbon metabolism, and increased reactive oxygen species (ROS) (Janka et al., 2013; Gu et al., 2017; Blackhall et al., 2020; Mihaljević et al., 2020). Studies have found that the synergistic effect of elevated temperature and high light caused significant degradation of D1 protein in plants, causing damage to both the donor and acceptor side of PSII (Krieger-Liszak et al., 2008; Kalaji et al., 2016). Sunburn occurs on leaves under the long-term high light, and sunspots were also found on some fruits, which seriously affects fruit quality and crop yield (Chen et al., 2012; Blackhall et al., 2020). Under natural conditions, heat and high light stress often occur simultaneously and tend to damage the photosynthetic apparatus of inverted leaves; nevertheless, the state of the photosynthetic system of inverted leaves under elevated temperature and high irradiation needs further study.

The rapid chlorophyll *a* fluorescence technique is a nondestructive and effective tool for monitoring the effects of abiotic stress on the photochemical efficiency of PSII and the health of the plant, because it quickly, noninvasively analyzes and provides powerful data related to photosynthesis (Strasser and Srivastava, 1995; Oukarroum et al., 2018). The typical rise in chlorophyll *a* fluorescence transient kinetics over 1 s is multiphase (OJIP curve), and the shape of the OJIP curve changes with the physiological condition of the plant, reflecting valuable information on the structure and function of the photosynthetic apparatus (Kalaji et al., 2016). Strasser et al. (2004) developed a data processing method (JIP-test) for rapid chlorophyll *a* fluorescence induction curves based on the theory of energy fluxes in thylakoid membranes. The specific flux of

each reaction center (RC) and the apparent flux of excited leaf cross-section (CS_O) provide rich information about the redox state of PSII (Strasser et al., 2010; Kalaji et al., 2016). The JIP-test has been widely used to analyze crop tolerance to single abiotic stresses and to screen for indicators of resistance identification, for example, elevated temperature stress (Janka et al., 2013; Mihaljević et al., 2020), nutrient deficiencies (Kalaji et al., 2014), drought stress (Marcińska et al., 2017), and high light stress (Hazrati et al., 2016).

Previous studies have shown that the photochemical efficiency of leaves is reduced when the leaf is inverted (Paradiso et al., 2020). In this study, we aimed to investigate the daily response of inverted leaves under specific conditions of high temperature and high irradiation at the photosynthetic level. We used JIP-test and gas exchange parameters to evaluate the photochemical adaptation of inverted leaves under elevated temperature and high light at noon. We hypothesized that PSII function is weaker and photochemical efficiency is lower in inverted leaves under high temperature and high light compared to normal leaves.

MATERIALS AND METHODS

Experimental Field and Meteorological Conditions

The field experiment was carried out in the Yili Institute of Agricultural Science in Xinjiang Production, China (43°50'N, 80°04'E). The experimental field was clay loam soil. The physicochemical properties of soil at 0–20 cm soil layer were as follows: available N 51.3 mg/kg, available P 15.8 mg/kg, and available K 102.1 mg/kg. For a better understanding of obtained results about the acclimatization of the photosynthetic apparatus of inverted leaves to heat and high light, we showed the data of air temperature and solar radiation measured on the day after treatment and recovery. The meteorological data were obtained from artificial weather devices placed in the test field as shown in **Figures 1A–D**. When the photosynthetic capacity of soybean leaves is measured, the temperature at 4 p.m. in summer is 38.2°C, and the light intensity is 1,512 $\mu\text{mol}(\text{CO}_2) \text{ m}^{-2} \text{ s}^{-1}$, which is much higher than its light saturation point.

Experimental Design

Spring soybean Heinong 87 from the Heilongjiang Academy of Agricultural Sciences of China (45° 58 N, 126° 48 E) was used as the experimental material. The experimental treatments consisted of leaf inversion treatment that the small middle leaves of four sections from the top of the plant were fixed with fine cotton thread and made to face up on the abaxial leaf surface during the seed-filling stage, then return to the original shape 15 days after the treatment, and do nothing for the control treatment. The experiment was conducted in a completely randomized block design and repeated three times. The plots were 4 m × 10 m. The soybean cultivar was sown with a density of 25.0 plants/m² on April 15, 2020 and 2021, the row spacing of 40 cm, and the plant spacing of 10 cm. Other management referred to local high-yield practices.

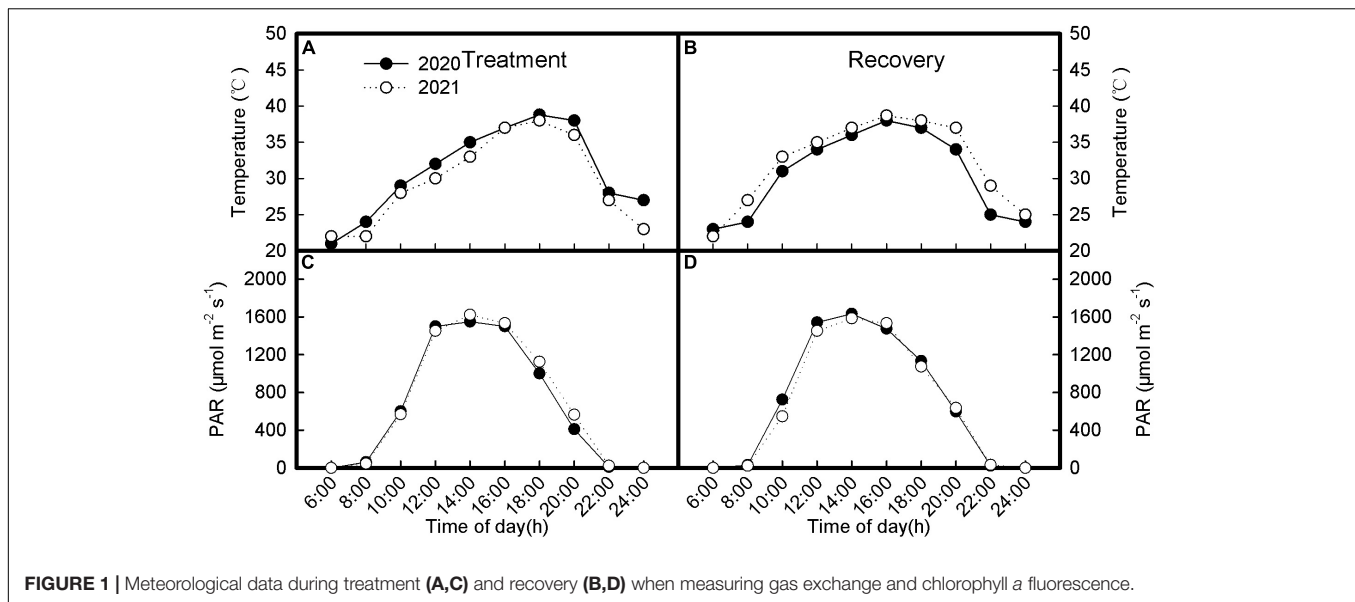


FIGURE 1 | Meteorological data during treatment (A,C) and recovery (B,D) when measuring gas exchange and chlorophyll *a* fluorescence.

Measurement of Photosynthetic Traits

We tried to choose the days with high temperature and solar radiation for measurement. The adaxial surface of fully expanded leaves in the main stem for both treatments was illuminated when they were inside the CIRAS chamber in both treatments. The net photosynthetic rate (P_n), transpiration rate (T_r), stomatal conductance (g_s), and intercellular carbon dioxide concentration (C_i) were measured from both treatments at 10 and 15 days (recovery) after leaf treatments, in the morning (9 a.m.) and afternoon (4 p.m.) using a portable photosynthesis system (CIRAS-3, PP Systems, London, United Kingdom). Steady-state photosynthesis was achieved after the leaves were clamped for 5 min, and the photosynthetic parameters were recorded at 1,800 $\mu\text{mol m}^{-2} \text{s}^{-1}$ light intensity, $400 \pm 5 \mu\text{mol mol}^{-1} \text{CO}_2$, and 70% humidity.

Photosynthetic Light-Response Curves

Photosynthetic light-response curves of fully expanded leaves in the main stem of soybean were measured 10 days after leaf inversion using a portable photosynthesis system (CIRAS-3, PP Systems, London, United Kingdom) between 11:00 a.m. and 1:30 p.m. at the soybean R5 expanding stage. The P_N was recorded at photosynthetic photon flux densities (PPFDs) of the following: 2,000; 1,800; 1,500; 1,200; 1,000; 800; 600; 400; 200; 150; 100; 50; 30; and 0 $\mu\text{mol m}^{-2} \text{s}^{-1}$, respectively. These measurements were recorded at a fixed CO_2 concentration of $400 \pm 5 \mu\text{mol mol}^{-1}$ using CO_2 cylinders. The photosynthetic light-response curves can be fitted with a nonlinear hyperbolic model (Farquhar et al., 1980) as follows:

$$P_N(I) = \frac{\alpha I + P_{N\max} - \sqrt{(\alpha I + P_{N\max})^2 - 4\alpha I P_{N\max}}}{2\theta} - R_D$$

where α is the apparent quantum yield (AQY), I represents the PPFD, $P_{N\max}$ is the maximum net photosynthetic rate,

R_D is the dark respiration rate, and θ is the convexity. The linear regression analysis was performed using SPSS version 19.0 software (IBM, Chicago, IL, United States) in the PPFD of 0–2,000 $\mu\text{mol m}^{-2} \text{s}^{-1}$. The crossover point of this line with the x-axis (photosynthetically active radiation, PAR) was the light compensation point (LCP, $\mu\text{mol m}^{-2} \text{s}^{-1}$), whereas the corresponding x-axis value for the crossover points along the y-axis was the light saturation point (LSP, $\mu\text{mol m}^{-2} \text{s}^{-1}$).

Chlorophyll *a* Fluorescence

The rapid chlorophyll *a* fluorescence induction kinetics were measured using a Plant Efficiency Analyzer (Handy-PEA, Hansatech, Norfolk, United Kingdom) at 9 a.m. and 4 p.m. 10 and 15 days after treatment. The leaves (from 10 individual plants) per treatment were dark-adapted using a fixing leaf clip (Hansatech) for 30 min. The samples were illuminated with 660-nm light of 3,000 photons $\mu\text{mol m}^{-2} \text{s}^{-1}$ for 1 s, and all the collected data were analyzed using the program plant efficiency analyser (PEA) Plus to obtain OJIP-test parameters (Kalaji et al., 2012), as shown in **Table 1**. To further analyze the difference in fluorescence kinetics between morning and afternoon measurements in response to elevated temperature and excess light, the original chlorophyll *a* fluorescence (OJIP) transients were normalized between minimum fluorescence when all PSII RCs were open (F_0) and maximum fluorescence when all PSII RCs were closed (F_m): the relative variable fluorescence was expressed as V_{OP} [$V_{OP} = (F_t - F_0)/(F_m - F_0)$], and the difference between the transients was expressed as ΔV_{OP} [$\Delta V_{OP} = V_{OP}(\text{measurement at 4 p.m.}) - V_{OP}(\text{measurement at 9 a.m.})$]. The original OJIP transients that were normalized between F_0 and F_K were expressed as V_{OK} [$V_{OK} = (F_t - F_0)/(F_K - F_0)$], between F_0 and F_J were expressed as V_{OJ} [$V_{OJ} = (F_t - F_0)/(F_J - F_0)$], between F_J and F_I were expressed as V_{JI} [$V_{JI} = (F_t - F_J)/(F_I - F_J)$], and between F_I and F_P were expressed as V_{IP} [$V_{IP} = (F_t - F_I)/(F_P - F_I)$];

TABLE 1 | Kinetic parameters of chlorophyll fluorescence.

	Fluorescence parameter	Description
Extracted parameter	$V_K=(F_{300\mu s}-F_0)/(F_m-F_0)$	Relative variable fluorescence at 300 μ s after illumination of a dark-adapted sample
	$V_J=(F_{2ms}-F_0)/(F_m-F_0)$	Relative variable fluorescence at 2 ms after illumination of a dark-adapted sample
	$V_I=(F_{30ms}-F_0)/(F_m-F_0)$	Relative variable fluorescence at 30 ms after illumination of a dark-adapted sample
	V_K/V_J	Limitation/inactivation and possibly damage of the oxygen-evolving complex
	Area	Density area over the chlorophyll a fluorescence transient delimited by a horizontal line at F_m
	F_0	Minimum fluorescence, when all PS II reaction center (RC) was open
	F_m	Maximum fluorescence, when all PS II RC was closed
	$F_V=F_m-F_0$	Maximum variable fluorescence
	$M_0=4(F_{300\mu s}-F_0)/(F_m-F_0)$	Approximated initial slope of the fluorescent transient. This parameter is related to rate of closure of reaction centers
	F_V/F_0	maximum ratio of quantum yields of photochemical and concurrent non-photochemical processes in PS II
Specific fluxes per RC	$RC/CS=F_0 \times \varphi_{PO} \times V_J/M_0$	Density of active RCs (Q_A reducing RCs) per cross section at point 0
	$ABS/RC=M_0 \times (1/V_J) \times [1-(F_0/F_m)]$	Absorption flux per RC
	$DI_0/RC=(ABS/RC)-(TR_0/RC)$	Dissipated energy flux per RC
	$TR_0/RC=M_0 \times (1/V_J)$	Trapped energy flux per RC
	$ET_0/RC=M_0 \times (1/V_J) \times \Psi_{EO}$	Electron transport flux per RC
	$RE_0/RC=(ET_0/RC) \times \delta_{RO}$	Reduction of end acceptors at PS I electron acceptor side per RC
	Yield or flux ratio	$\varphi_{PO}=F_V/F_m$
$\Psi_{EO}=ET_0/TR_0=1-V_J$		Probability that a trapped exciton moves an electron into the trapped electron transport chain beyond Q_A^-
$\varphi_{EO}=(F_V/F_m) (1-V_J)$		Quantum yield for electron transport at $t = 0$
$\delta_{RO}=(1-V_I) (1-V_J)$		Efficiency with which an electron can move from the reduced intersystem electron acceptors to the PS I end electron acceptors
$\varphi_{RO} = \varphi_{PO} \times \Psi_{EO} \times \delta_{RO}$		Quantum yield for the reduction of end acceptors of PS II per photon absorbed
Performance index (PI)		$PI_{ABS}=(RC/ABS)[\varphi_{PO}/(1-\varphi_{PO})][\Psi_{EO}/(1-\Psi_{EO})]$
	$PI_{total}=PI_{ABS} \times \delta_{RO}/(1-\delta_{RO})$	Total PI, measuring the performance up to the PS I end electron acceptors

finally, the differences between the transients which were expressed as ΔV_{OK} [$\Delta V_{OK} = V_{OK}(\text{measurement at 4 p.m.}) - V_{OK}(\text{measurement at 9 a.m.})$], ΔV_{OJ} [$\Delta V_{OJ} = V_{OJ}(\text{measurement at 4 p.m.}) - V_{OJ}(\text{measurement at 9 a.m.})$], ΔV_{JI} [$\Delta V_{JI} = V_{JI}(\text{measurement at 4 p.m.}) - V_{JI}(\text{measurement at 9 a.m.})$], ΔV_{IP} [$\Delta V_{IP} = V_{IP}(\text{measurement at 4 p.m.}) - V_{IP}(\text{measurement at 9 a.m.})$], and ΔV_{OP} [$\Delta V_{OP} = V_{OP}(\text{measurement at 4 p.m.}) - V_{OP}(\text{measurement at 9 a.m.})$] were determined for visualization (Li et al., 2020).

Data Analysis

The PEA Plus software was used to obtain the OJIP-test parameters. The differences between data at the two measurement time points (morning and afternoon) and between leaf treatments were analyzed by one-way ANOVA with the SPSS version 19.0 (SPSS Inc., Chicago, IL, United States). The structures of variability and correlations between the measured parameters were explored by the principal component analysis (PCA), the selection of the principal factors was based on those with eigenvalues greater than 1. The data are presented as the mean \pm SE, and the means were compared using least significant difference (LSD) tests, $*P < 0.05$ and $**P < 0.01$. The graphs were constructed using SigmaPlot software, version 12.5.

RESULTS

Leaf Gas Exchange

As shown in **Figures 2A,B**, the P_n , gs, and C_i values of normal and inverted leaves (except C_i values for inverted leaves in 2020) were significantly reduced at noon during treatment compared with those measured in the morning ($P < 0.05$), and the decline was higher for inverted leaves than for normal leaves; T_r values for inverted leaves were significantly lower ($P < 0.05$) than for normal leaves at noon measurements, and the T_r values of the normal leaves was not significantly different between 9 a.m. and 4 p.m. ($P > 0.05$), while inverted leaves decreased significantly at 4 p.m. compared to the 9 a.m. measurement ($P < 0.05$). After recovery of inverted leaves, the P_n and gs values of all treated leaves showed the same trend as leaves during treatment; C_i and T_r values of normal and inverted leaves were elevated at noon compared to morning measurements, with higher C_i values of inverted leaves than normal leaves, but the opposite for T_r values.

Photosynthetic Light-Response Curves

The ANOVA showed that P_{Nmax} , AQY, R_D , LCP, and LSP were affected by leaf inversion ($P < 0.05$) when the leaf was inverted and restored (**Table 2**). During leaf inversion, P_{Nmax} , AQY, R_D , LCP, and LSP of inverted leaves were reduced by 59.1%, 51.2%, 49.1%, 16.5%, and 13.1%, respectively, compared to normal leaves. After the inverted leaves recovered, the P_{Nmax} , AQY, R_D , LCP, and LSP of the leaves were reduced by 33.2%, 25.2%, 19.4%, 1.9%, and 16.0%, respectively, compared to the normal leaves.

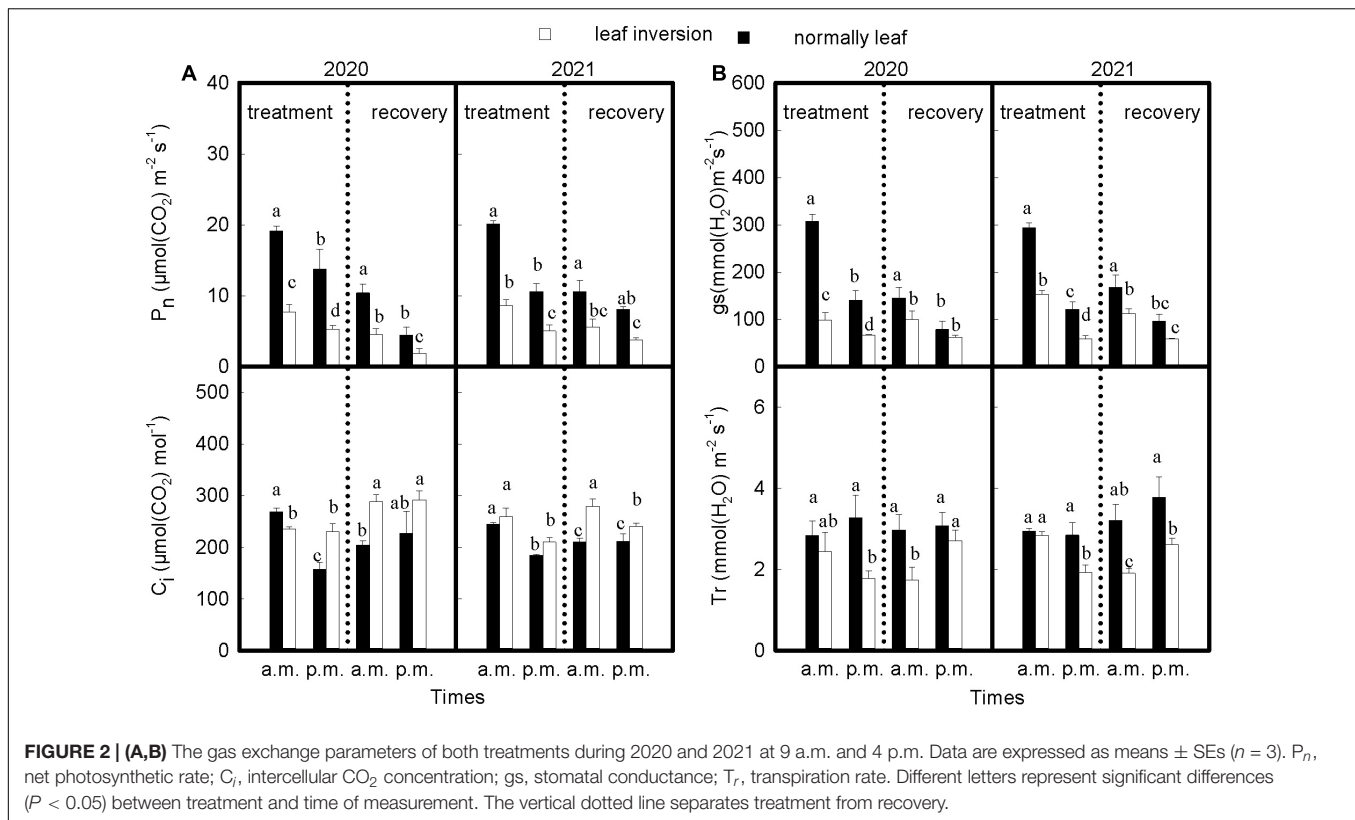


TABLE 2 | Photosynthetic light-response parameters of inverted leaves in 2021.

Times	Treatment	P_{Nmax} [$\mu\text{mol}(\text{CO}_2)$ $\text{m}^{-2} \text{s}^{-1}$]	R_D [$\mu\text{mol}(\text{CO}_2)$ $\text{m}^{-2} \text{s}^{-1}$]	AQY [$\text{mol}(\text{CO}_2)$ $\text{mol}^{-1}(\text{photon})$]	LCP [$\mu\text{mol}(\text{CO}_2)$ $\text{m}^{-2} \text{s}^{-1}$]	LSP [$\mu\text{mol}(\text{CO}_2)$ $\text{m}^{-2} \text{s}^{-1}$]
Treatments	CK	31.7 ± 1.2^a	6.7 ± 0.2^a	0.057 ± 0.001^a	130.1 ± 1.3^a	664.7 ± 12.1^a
	Leaf inversion	13.0 ± 1.5^b	3.3 ± 0.5^b	0.029 ± 0.002^b	108.7 ± 1.9^b	577.3 ± 11.4^b
Recovery	CK	17.4 ± 0.6^a	5.9 ± 0.4^a	0.036 ± 0.001^a	130.5 ± 1.4^a	629.6 ± 13.4^a
	Leaf inversion	11.6 ± 1.1^b	4.4 ± 0.3^b	0.029 ± 0.001^b	128.0 ± 2.1^a	528.4 ± 15.3^b

P_{Nmax} , the maximum net photosynthetic rate; R_D , dark respiration rate; AQY, apparent quantum yield; LCP, light compensation point; LSP, light saturation point. Different letters indicate a statistically significant level at $P < 0.05$. Bars mean SE ($n = 3$).

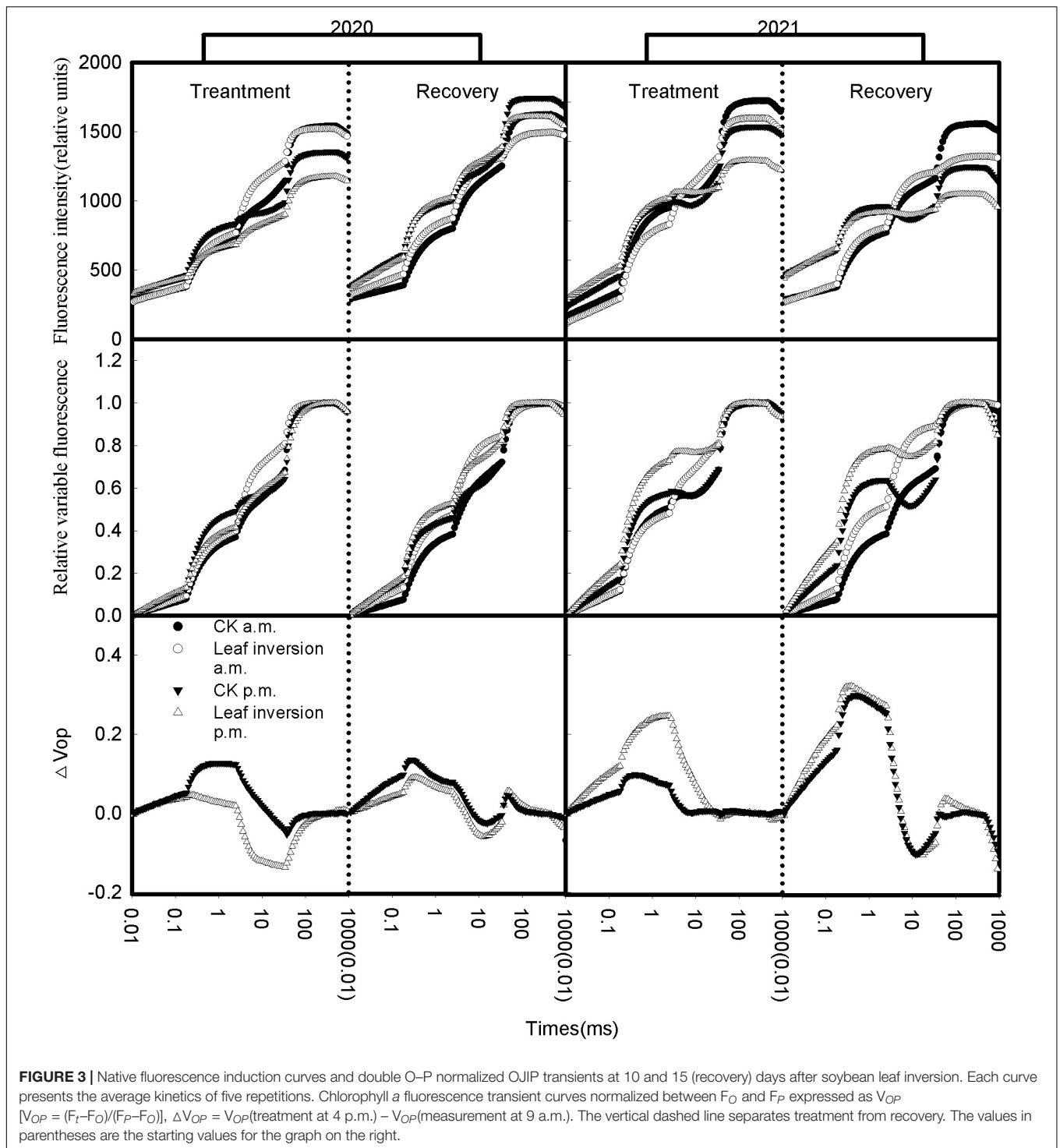
Chlorophyll a Fluorescence Rise

When the chlorophyll *a* fluorescence induction curves were plotted on the logarithmic timescale as the horizontal coordinate and the immediate chlorophyll *a* fluorescence intensity of all treated leaves as the vertical coordinate, a rapid rise in the OJIP fluorescence transient was evident (Figure 3). Both the measurement at 4 p.m. and the leaf inversion resulted in a change in the shape of the chlorophyll *a* fluorescence induction curve, and when the inverted leaves were restored, the shape of the chlorophyll *a* fluorescence induction curve did not change. To further evaluate the changes in leaf photosynthetic performance under heat and high light at noon, a relative variable fluorescence curve [$V_{OP} = (F_t - F_0)/(F_m - F_0)$] was constructed to compare the differences in plant photosynthetic performance between 4 p.m. and 9 a.m. The value of each difference curve was the relative variable fluorescence value recorded at 4 p.m. minus the relative variable fluorescence value recorded at 9 a.m.

[$\Delta V_{OP} = V_{OP}(\text{measurement at 4 p.m.}) - V_{OP}(\text{measurement at 9 a.m.})$]. The shape of the relative variable fluorescence curve of leaves recorded at 4 p.m. differed from that recorded at 9 a.m. In all treatments, changes in fluorescence transient curve shape caused by elevated temperature and high light could be clearly visualized by difference curves. In 2020, the difference curves for inverted leaves have a larger magnitude of variation compared to normal leaves, while in 2021 the difference curves for normal leaves have a larger magnitude of variation.

Normalization of Chlorophyll a Fluorescence Transient Curves

To further elucidate the differences between treatments during the O-P phase of the chlorophyll *a* fluorescence transient, we, respectively, presented the differential curves for the main bands occurring during the O-P transient. The curves for these bands were constructed by subtracting the standardized fluorescence



values of plants recorded at 4 p.m. (between O and K, O and J, J and I, or I and P, respectively) from the standardized fluorescence values of plants recorded at 9 a.m. (Figures 4A–D). The O–K normalized curve, called the L-band, provides information on the effective light absorption and energy utilization in the initial phase of photosynthesis. The leaves showed positive L-bands for all groups caused by elevated temperature and high light at 4

p.m. during treatment and recovery; the O–J normalized curve called K-band was used to check the status of the PSII donor side, where heat and high light at 4 p.m. caused all groups to show positive K-bands. The J–I normalized and I–P normalized curves indicate the balance between reduction and oxidation of the Q_A and plastoquinone (PQ) pools, respectively, and the J–I normalized curves showed a difference between years and

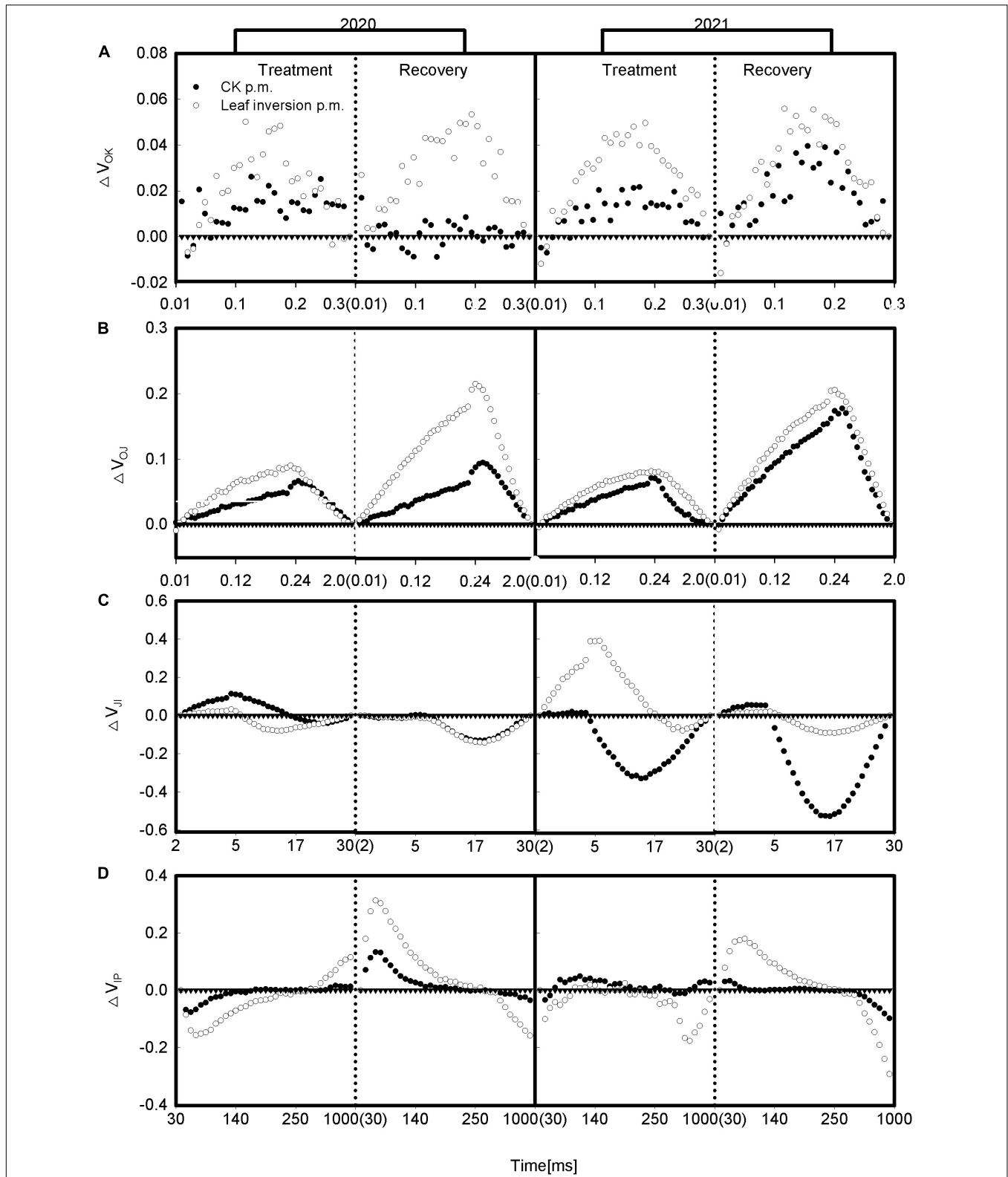
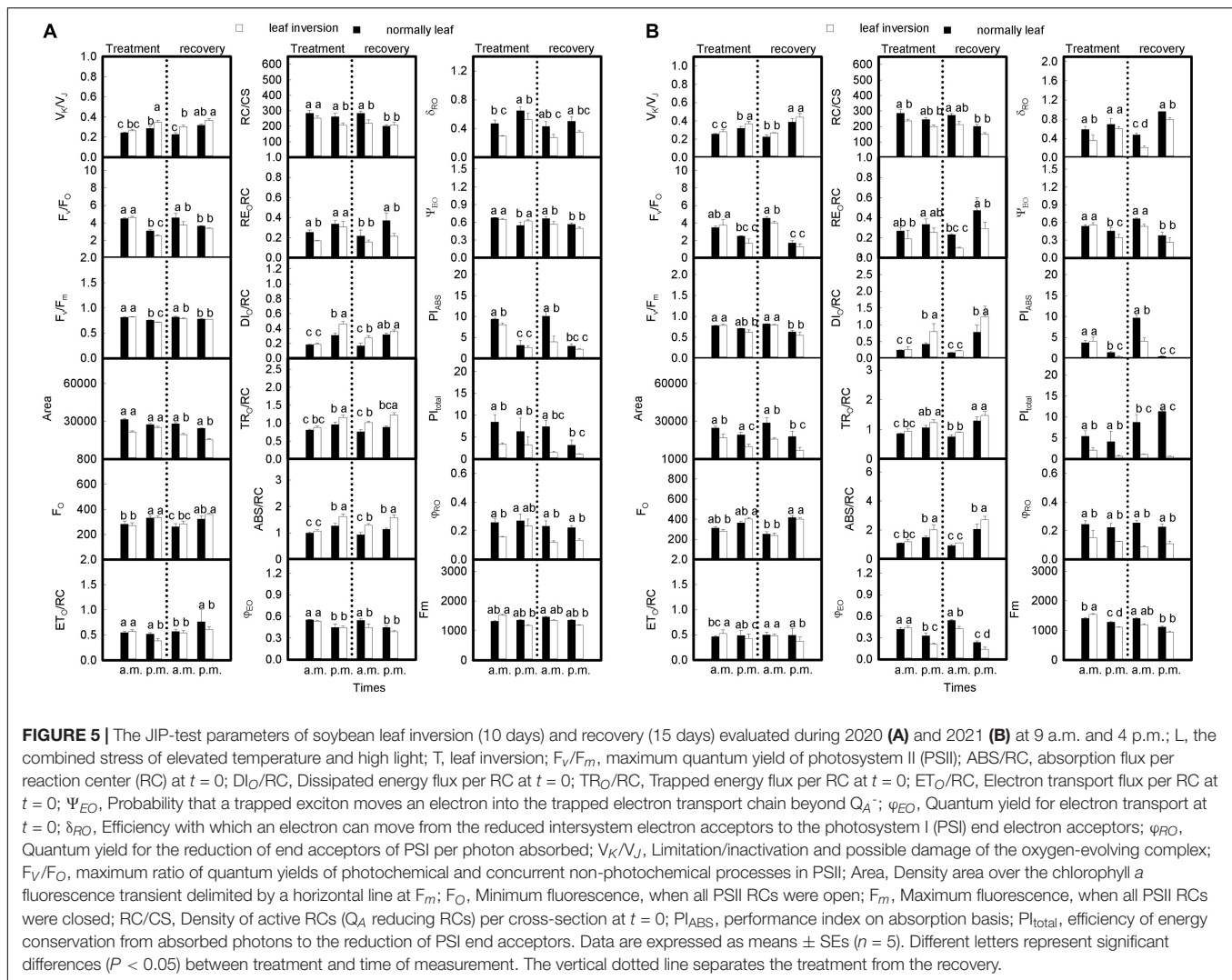


FIGURE 4 | (A–D) Double normalization between F_O and F_K expressed as V_{OK} [$V_{OK} = (F_t - F_O)/(F_K - F_O)$], between F_O and F_j expressed as V_{Oj} [$V_{Oj} = (F_t - F_O)/(F_j - F_O)$], between F_j and F_i expressed as V_{ji} [$V_{ji} = (F_t - F_j)/(F_i - F_j)$], and between F_i and F_P expressed as V_{IP} [$V_{IP} = (F_t - F_i)/(F_P - F_i)$]. $\Delta V_{OX} = V_{OX}(\text{measurement at 4 p.m.}) - V_{OX}(\text{measurement at 9 a.m.})$. Each curve presents the average kinetics of five repetitions. The vertical dotted line separates treatment from recovery. The values in parentheses are the starting values for the graph on the right.



treatments, with inverted leaves showing negative bands during treatment in 2020, while normal leaves showed positive bands and inverted leaves still showed negative bands after recovery, 2021 and 2020 were exactly the opposite, with leaves showing the highest negative bands during treatment and recovery. The I-P normalization curves differed between treatments, with inverted leaves showing a negative band during treatment and a positive band during recovery.

Specific Fluxes per Reaction Center and Flux Ratios

During the leaf treatment (Figures 5A,B and Table 3), the limitation/inactivation and possible damage of the oxygen-evolving complex (OEC) (V_K/V_J), RE_O/RC , dissipated energy flux per RC at $t = 0$ (DI_O/RC), trapped energy flux per RC at $t = 0$ (TR_O/RC), absorption flux per RC (ABS/RC), efficiency with which an electron can move from the reduced intersystem electron acceptors to the photosystem I (PSI) end electron acceptors (δ_{RO}), and minimum fluorescence when all PSII RCs

were open (F_O) values increased at 4 p.m. for inverted and normal leaves compared to measurements at 9 a.m., while F_V/F_O , F_V/F_m , Area, electron transport flux per RC at $t = 0$ (ET_O/RC), the density of active RCs (Q_A reducing RCs) per cross-section at $t = 0$ (RC/CS), quantum yield for electron transport at $t = 0$ (ϕ_{EO}), the probability that a trapped exciton moves an electron into the trapped electron transport chain beyond Q_A^- (Ψ_{EO}), PI_{total} , quantum yield for the reduction of end acceptors of PSI per photon absorbed (ϕ_{RO}), and F_m values decreased at 4 p.m. When inverted leaves recovered, the trend in values was consistent with the leaves during treatment except for ET_O/RC and PI_{total} values; compared to measurements at 9 a.m., ET_O/RC values increased at 4 p.m. after inverted leaves recovered in 2020, but the difference was not significant, but significantly decreased in 2021; PI_{total} values decreased at 4 p.m. for all groups in 2020, but in 2021 normal leaves increased slightly at 4 p.m. Leaf V_K/V_J , RC/CS , RE_O/RC , DI_O/RC , ABS/RC , δ_{RO} , PI_{ABS} , and PI_{total} values differed significantly ($P < 0.05$) between measurements at 9 a.m. and 4 p.m. during treatment, and their values also showed significant differences ($P < 0.05$) between inverted and normal

leaves; F_v/F_o , F_o , F_m , and ET_o/RC values were significantly different between 9 a.m. and 4 p.m. measurements ($P < 0.05$), while leaf inversion did not affect their values significantly ($P > 0.05$); ϕ_{RO} values were not significantly different between 9 a.m. and 4 p.m. measurements ($P > 0.05$), but leaf inversion affected their values significantly ($P < 0.05$); F_v/F_m , TR_o/RC , ϕ_{EO} , and Ψ_{EO} values were significantly different between 9 a.m. and 4 p.m. measurements ($P < 0.05$); F_v/F_m , TR_o/RC , ϕ_{EO} , and Ψ_{EO} values were significantly different between 9 a.m. and 4 p.m. measurements. F_v/F_m , TR_o/RC , ϕ_{EO} , and Ψ_{EO} values were significantly different between 9 a.m. and 4 p.m. measurements ($P < 0.05$), and leaf inversion had no effect or reached a significant level. There was no significant difference in the Area value measured at 9 a.m. and 4 p.m. in 2020 ($P > 0.05$), and leaf inversion had no effect on its value, but there was a significant difference between the treatment groups in 2021 ($P < 0.05$). PI_{ABS} and PI_{total} were significantly lower ($P < 0.05$) for the 4 p.m. measurement compared to the 9 a.m. measurement. The interaction of leaf inversion and time of measurement on chlorophyll *a* fluorescence parameters in both years was not significant only for V_K/V_J , ET_o/RC , RE_o/RC , PI_{ABS} , F_o , TR_o/RC , RC/CS , δ_{RO} , and ϕ_{RO} .

After leaf inversion recovery (Figures 5A,B and Table 3), leaf V_K/V_J , ET_o/RC , RE_o/RC , DI_o/RC , ABS/RC , ϕ_{EO} , Ψ_{EO} , PI_{ABS} , and PI_{total} values differed significantly ($P < 0.05$) between the 9 a.m. and 4 p.m. measurements, and their values also showed significant differences ($P < 0.05$) between inverted and normal leaves; F_v/F_o , F_o , F_m , F_v/F_m , Area, and TR_o/RC values differed significantly ($P < 0.05$) between the 9 a.m. and 4 p.m. measurements, while the effect of leaf inversion on their values varied from year to year; RC/CS , δ_{RO} , and ϕ_{RO} values differed significantly ($P < 0.05$) between the 9 a.m. and 4 p.m. measurements, and the effect of leaf inversion on their values varied from year to year. The interaction of leaf inversion and time of measurement on other chlorophyll *a* fluorescence parameters was not significant in both years except for Area, PI_{ABS} , and PI_{total} values.

Principal Component Analysis

The PCA of the fluorescence and gas exchange parameters of the examined soybean cultivars revealed both differences and similarities between the different treatments (Table 4 and Figure 6), with the first 2 principal components (PCs) accounting for 79.0%–96.6% of the total variance. Leaves were treated with the first PC (PC1) reflecting 50.8% and 65.9% of the total variance in 2020 and 2021, respectively, and the second PC (PC2) reflecting 28.2% and 29.8% of the total variance, respectively. The results of PCA indicated that normal leaves measured at 9 a.m. exhibited higher photosynthesis (P_n), performance indexes (PI_{total} and PI_{ABS}), and number of RCs (RC/CS); inverted leaves measured at 4 p.m. were characterized by higher specific activity parameters (ABS/RC , DI_o/RC , and TR_o/RC), while normal leaves had higher loads on Area, δ_{RO} , and RE_o/RC . After inverted leaf recovery, the PC1 reflected 68.4% and 62.7% of the total variation in 2020 and 2021, respectively, and the PC2 reflected 27.2% and 33.9% of the total variation, respectively. Normal leaves measured at 9 a.m. in 2020 and 4 p.m. in 2021 exhibited

TABLE 3 | ANOVA of effects of elevated temperature and high light stress on fluorescence parameters.

Treatments	Source of variation	2020												2021											
		V_K/V_J	F_v/F_o	F_v/F_m	Area	F_o	ET_o/RC	RC/CS	RE_o/RC	DI_o/RC	TR_o/RC	ABS/RC	ϕ_{EO}	δ_{RO}	Ψ_{EO}	PI_{ABS}	PI_{total}	ϕ_{RO}	F_m						
Leaf version	L	**	*	**	ns	*	*	**	**	**	**	**	**	**	**	**	ns	ns	*						
	T	**	ns	*	ns	ns	**	*	**	**	**	ns	*	ns	**	**	*	ns	ns						
	L×T	ns	*	**	ns	ns	ns	ns	ns	ns	*	*	ns	ns	ns	ns	ns	ns	*						
Recovery	L	**	*	*	*	**	ns	*	**	**	**	*	ns	ns	**	**	ns	ns	*						
	T	**	ns	*	ns	ns	**	*	**	**	**	*	**	*	*	*	**	**	*						
	L×T	ns	ns	ns	**	ns	ns	ns	ns	ns	ns	ns	ns	ns	ns	*	*	ns	ns						
Leaf version	L	**	**	**	**	*	*	*	**	**	**	*	*	**	**	*	*	ns	**						
	T	*	ns	ns	**	ns	*	*	**	ns	*	*	*	**	*	*	**	**	ns						
	L×T	ns	ns	ns	ns	ns	ns	ns	ns	ns	ns	ns	ns	ns	ns	ns	ns	ns	**						
Recovery	L	**	**	**	**	**	*	*	**	**	**	*	*	**	**	*	*	ns	*						
	T	*	*	ns	**	ns	*	*	*	*	*	*	*	**	*	*	*	**	*						
	L×T	ns	ns	ns	ns	ns	ns	ns	ns	ns	ns	ns	ns	ns	ns	**	**	ns	ns						

L, Light treatment; T, temperature treatment. ** significantly different at $P < 0.01$; * significantly different at $P < 0.05$; ns, the difference was not significant.

TABLE 4 | The results of principal component analysis (PCA).

Year		2020				2021			
Different measures		Treatments		Recovery		Treatments		Recovery	
Principle factors		PC1	PC2	PC1	PC2	PC1	PC2	PC1	PC2
Eigen vector	RC/CS	-0.782	0.623	0.978	-0.080	0.796	0.524	0.935	0.349
	V_K/V_J	0.901	-0.403	-0.940	0.340	-0.991	-0.070	-0.997	0.040
	Area	0.058	0.997	0.777	0.600	0.825	0.565	0.854	0.511
	F_v/F_m	-0.933	0.133	0.992	0.116	0.990	-0.034	0.979	-0.196
	F_v/F_o	-0.907	0.083	0.993	0.115	0.987	-0.150	0.975	-0.213
	Sm	0.860	0.476	0.849	0.422	0.592	0.804	0.486	0.860
	N	0.983	0.059	-0.358	0.819	-0.026	0.952	-0.367	0.870
	ABS/RC	0.926	-0.330	-0.952	0.307	-0.998	-0.058	-0.989	0.066
	DI _O /RC	0.949	-0.242	-0.975	0.216	-0.990	-0.050	-0.980	0.086
	TR _O /RC	0.901	-0.402	-0.940	0.340	-0.991	-0.069	-0.997	0.040
	ET _O /RC	0.824	-0.438	-0.768	0.604	0.781	-0.058	0.831	0.355
	(RE _O)/RC	0.901	0.240	-0.358	0.934	-0.209	0.962	-0.505	0.858
	Ψ_{Eo}	-0.280	0.036	0.948	0.249	0.984	-0.027	0.998	0.058
	φ_{Eo}	-0.632	0.095	0.963	0.222	0.987	-0.062	0.999	-0.027
	δR_o	0.563	0.518	0.079	0.975	-0.531	0.841	-0.717	0.695
	φR_o	0.447	0.828	0.508	0.853	0.530	0.848	0.388	0.906
	PI _{ABS}	-0.759	0.224	0.994	0.048	0.976	-0.211	0.929	0.046
	PI _{total}	-0.336	0.937	0.921	0.342	0.728	0.648	0.271	0.951
	T _r	-0.558	0.577	0.136	0.802	0.660	0.750	-0.100	0.994
g _s	-0.356	0.872	0.991	0.003	0.944	0.225	0.957	0.255	
P _n	-0.402	0.915	0.977	0.206	0.855	0.453	0.725	0.683	
C _i	-0.120	0.094	-0.671	-0.740	0.489	-0.860	0.004	-0.936	
Eigenvalues		13.283	5.982	15.139	5.907	14.976	6.086	13.931	7.321
Variation explained (%)		50.815	28.220	68.432	27.232	65.894	29.842	62.730	33.870
Cumulative proportion (%)		50.815	79.035	68.432	95.665	65.894	95.737	65.894	96.600

Vector loadings ≥ 0.90 are mentioned in bold.

higher P_n , performance indexes (PI_{total} and PI_{ABS}), and number of RCs (RC/CS). P_n was positively correlated with PI_{ABS}, PI_{total}, and RC/CS and negatively correlated with ABS/RC, DI_O/RC, and TR_O/RC.

DISCUSSION

Under natural conditions, a combination of high light and heat stress in summer is the main environmental stress that leads to a decrease in plant photosynthesis, usually starting with a reduction in the production of photosynthetic assimilates under mild abiotic stress when leaves avoid water dissipation by reducing stomatal aperture and thus limiting the mesophyll conductance to CO₂, at which point diffusive limitation is the main cause of the decrease in leaf photosynthetic capacity (Das et al., 2015; Bahamonde et al., 2018; Fanourakis et al., 2019; Mihaljević et al., 2020). As the stress level increased and time increased, the leaf photosynthetic apparatus was damaged and PSII photochemical activity was reduced in addition to diffusive limitation, and at this time, the nondiffusion limitation was better than diffusion limitation (Hazrati et al., 2016; Jiang et al., 2021). In this study, the P_n and g_s of inverted leaves and normal leaves

were significantly reduced at 4 p.m. during the treatment, and C_i of normal leaves was also significantly reduced at noon, but C_i in inverted leaves behaved differently in both years, with no significant difference between 9 a.m. and 4 p.m. C_i in inverted leaves in 2020, while the difference reached a significant level in 2021, which could be caused by climatic factors between years but could at least suggest that the reduction in P_n of normal leaves can be explained by a reduction in g_s (Pandey et al., 2007) and that inverted leaves may be more susceptible to photooxidative damage and damage to the photosynthetic apparatus at elevated temperature and high light compared to normal leaves, which is supported by the decrease in F_v/F_m values and performance indexes (PI_{ABS} and PI_{total}) and the increase in DI_O/RC values in inverted leaves at noon. Between the 2 years, the T_r values of normal leaves were slightly elevated or flat in the noon compared to the morning measurement, but T_r values of inverted leaves were significantly lower in the noon, which may also be one of the reasons for the lower P_n of inverted leaves compared to normal leaves, as the lower transpiration rate leads to higher leaf temperature, and the photoinhibition of photosynthesis depends on Temperature, the increase of leaf temperature will strengthen the photoinhibition, thereby greatly reducing the photosynthetic capacity of inverted leaves (Avola et al., 2008; Das et al., 2015;

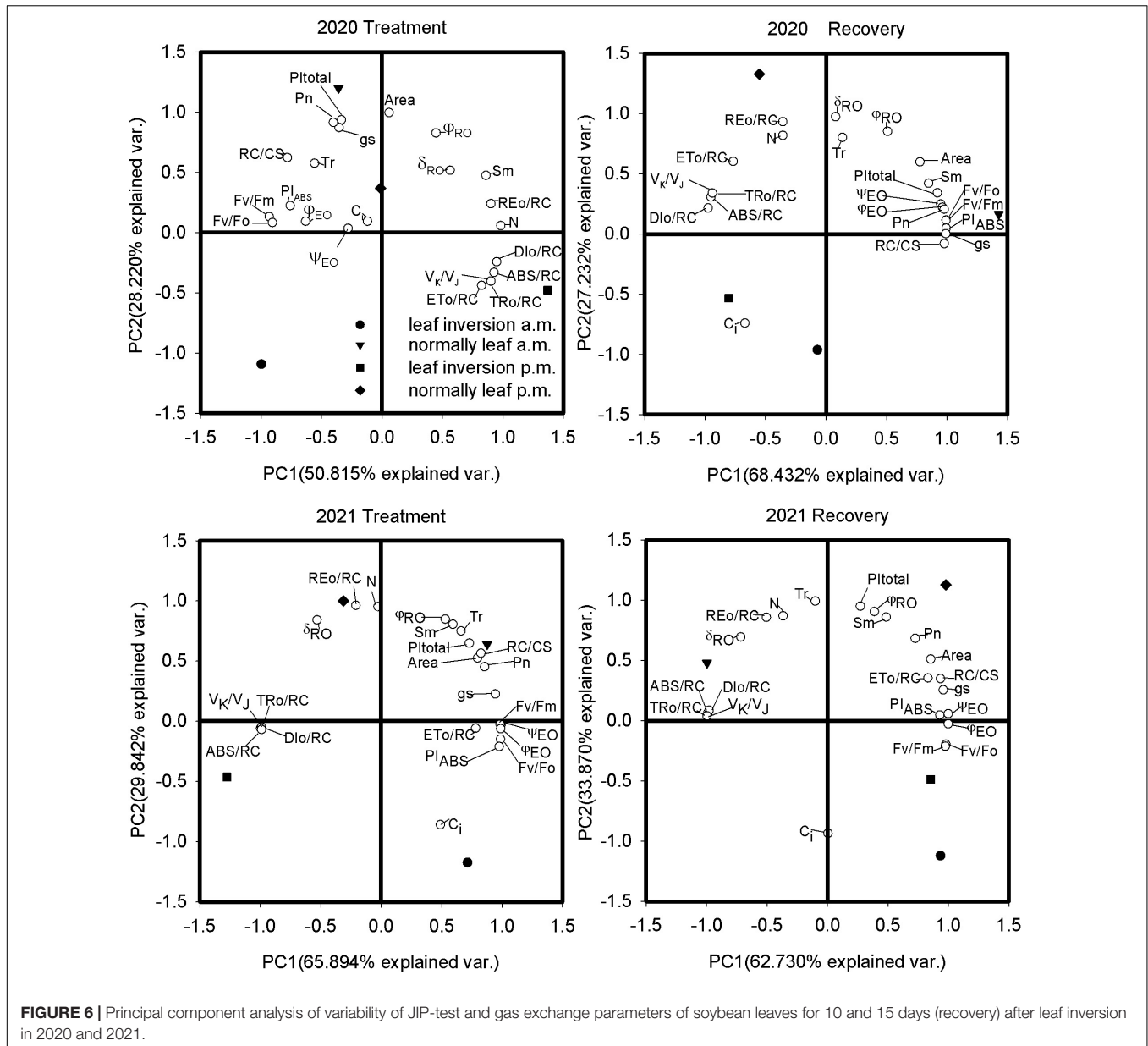


FIGURE 6 | Principal component analysis of variability of JIP-test and gas exchange parameters of soybean leaves for 10 and 15 days (recovery) after leaf inversion in 2020 and 2021.

Gago et al., 2015; Durand et al., 2020). After the recovery of inverted leaves, the C_i values of normal and inverted leaves did not decrease with the decrease of P_n and g_s values under elevated temperature and high light, and the C_i values of inverted leaves were higher than those of normal leaves, indicating that the irreversible damage to the photosynthetic apparatus of inverted leaves occurred under heat and high light (Mihaljević et al., 2020; Cohen et al., 2021), but the factor of shorter recovery time of inverted leaves could not be ignored. To obtain the adaptation of inverted leaves to light under the combined stress of high light and elevated temperature, the response of P_n to several light intensities of PPFD was evaluated. In this study, the P_{Nmax} , AQY, R_D , LCP, and LSP values of inverted leaves were lower than those of normal leaves under treatment and

recovery conditions, indicating that the photosynthetic potential of leaves under elevated temperature and high light was reduced and the ability to utilize strong light was weakened in inverted leaves, similar to the studies by Proietti and Palliotti (1997), Xu et al. (2013), and Paradiso et al. (2020). It is worth noting that the P_{Nmax} of normal leaves decreases significantly from treatment to recovery, and this may be due to the fact that soybeans are susceptible to high temperature stress during the filling stage, which induced and accelerated the senescence of inverted leaves in advance (i.e., PI_{total} of inverted leaves was significantly lower than that of normal leaves under elevated temperature and high light), while the photosynthetic products of normal leaves efficiently transport to the reproductive organs during the recovery phase, accelerating leaf senescence, resulting

in that the P_{Nmax} of the normal leaves was significantly lower during the recovery.

Many studies have assessed the harmful effects of heat on photosynthesis, where elevated temperatures reduce CO_2 fixation by inhibiting photosynthetic system activity. The inactivation of PSII in plants under complex stress in summer leads to a decrease in photosynthetic capacity (Fanourakis et al., 2019; Jiang et al., 2021). Some researchers have noted that F_v/F_m values of normal leaves range from 0.75 to 0.83 and that a decrease in this parameter indicates that PSII has been damaged (Krause and Weis, 1991). According to a certain one, an increase in F_o is one of the signs of photoinhibition (Uhrmacher et al., 1995). It has also been suggested that an increase in DI_o/RC and a decrease in Ψ_{EO} can be prepared to identify photoinhibition rather than F_v/F_m (Jiang et al., 2008). In this study, the F_v/F_m values of normal and inverted leaves were significantly lower at 4 p.m. compared to morning measurements, and the decrease was higher in inverted leaves than that of normal leaves. The F_v/F_m values ranged from 0.62 to 0.71 at 4 p.m. during treatment for inverted leaves, while normal leaves ranged from 0.71 to 0.75; after recovery of inverted leaves, the F_v/F_m of the inverted leaves in 2021 decreased significantly at 4 p.m. ($F_v/F_m = 0.55$) and that of the normal leaves is 0.61. At the same time, compared with the morning measurement, the F_v/F_m and Ψ_{EO} values of the inverted leaves decreased at 4 p.m., and the increase in DI_o/RC and F_o values were higher than those of the normal leaves. The LSP of the inverted leaf is between 528.4 and 577.3 $\mu mol(CO_2) m^{-2} s^{-1}$, while the normal leaf is between 629.6 and 664.7 $\mu mol(CO_2) m^{-2} s^{-1}$, and the temperature at 4 p.m. in summer is 38.2°C, and the light intensity is 1,512 $\mu mol(CO_2) m^{-2} s^{-1}$, which is much higher than its light saturation point, which causes the light system to be overexcited. All the above mentioned results indicate that the combined stress of elevated temperature and high light in summer promotes PSII inhibition of inverted leaves and stronger energy dissipation. This is supported by the significant increase in DI_o/RC value at 4 p.m. and the PCA results. This is similar to the study by Mihaljević et al. (2020) on apples.

In recent years, there has been considerable interest in using chlorophyll *a* fluorescence and related parameters to assess the effects of abiotic stress on the photosynthetic structure, using chlorophyll *a* fluorescence kinetics to characterize plant tolerance to abiotic stresses at the PSII level (Hussain et al., 2019; Rastogi et al., 2020). In fact, elevated temperature and high light stress result in significant changes in the shape of the chlorophyll fluorescence induction curve (Mihaljević et al., 2020). In this study, the combined high light and elevated temperature stresses significantly affected PSII performance during treatment and recovery of leaves, and these effects were visible in the variable fluorescence curves and relative variable fluorescence curves during treatment and recovery (Figures 3, 4). The typical shape of the OJIP transient curve has 3 main phases, namely, O-J, J-I, and I-P (Strasser and Srivastava, 1995). The J-I phase reflects the reduction of electron carriers (plastoquinone and plastocyanin) between PSII and PSI (Tóth et al., 2007). In this study, the increase in J-I transients in normal and inverted leaves differed by year, and an increase in J-I transients was observed in inverted leaves compared to normal leaves, which

supports the vulnerability of the electron carriers of the inverted leaves to elevated temperature and high light and the partial reduction of the PQ pools between PSII to PSI, which is consistent with the reduction in the PQ pools under elevated temperature reported by Mihaljević et al. (2020). The I-P phase is the slowest fluorescence rise and is associated with a decrease in electron transport proteins (Ceppi et al., 2012). Previous studies have confirmed that I-P is relatively sensitive to various abiotic stress (Schansker et al., 2005). In this study, inverted leaves showed a significant positive peak change during recovery, suggesting that damage to the PSI structure, loss of function in inverted leaves, and electron transport on the PSI receptor side may have been inhibited.

The PSII and OEC are one of the main stress-sensitive sites in the photosynthetic apparatus (Adamski et al., 2011). Previous studies have shown that high light and elevated temperature reduce PSII activity and electron transfer efficiency (Boguszewska-Mańkowska et al., 2018). In this study, the active RC of normal and inverted leaves was significantly reduced at 4 p.m. (supported by the increase in ABS/RC). The increase in ABS/RC may be due to the increase in antenna size or partial PSII RC inactivation, which can be confirmed by a decrease in active RC per excitation cross-section (RC/CS). The inactivation of RC is considered to be a photoprotective mechanism, because part of the RC is transformed into a so-called “heat sink” by Stefanov et al. (2011), to dissipate excess excitation energy to prevent excessive excitation of PSII. The significant increase in dissipated energy (DI_o/RC) supports the change of RC function. Compared with the morning measurement, the TR_o/RC and DI_o/RC of the inverted leaves increased by 31.5% and 135.1%, respectively, at 4 p.m., while the normal leaves increased by 21.4% and 39.1%, respectively. These findings suggest that inverted leaves dissipate excitation energy in the form of more heat and fluorescence and more severe photoinhibition, which is consistent with the research results of Mihaljević et al. (2020). ET_o/RC describes the electron transport flux of each RC, which reflects the activity of active RCs. The ET_o/RC values decreased at 4 p.m., but some researchers have shown that ET_o/RC values increased at elevated temperatures (Faria-Silva et al., 2019; Mihaljević et al., 2020). In this study, the ET_o/RC values of inverted leaves decreased significantly at 4 p.m. compared with 9 a.m., while normal leaves remained essentially unchanged, which further supports the hypothesis that some of the RC is converted into a “heat sink” and also indicates that the activity of active RC in inverted leaves is reduced under high light and elevated temperature, which is consistent with the study by Mihaljević et al. (2020). Elevated temperature and high light also affect both the donor and acceptor sides of PSII (Buchner et al., 2015): on the donor side, OEC inactivated, as shown in this study by a significant increase in the positive K-band at 300 ms and V_K/V_J , which may be due to the loss of manganese cluster function in PSII at elevated temperature, resulting in an imbalance electron transport between the OEC and the PSII RC; while at the acceptor site, the electron transport between Q_A^- and Q_B^- is inhibited (Gu et al., 2017), and the disruption of the electron transport chain is due to the dissociation of the LHCII from PSII, which

helps to avoid excessive reduction of PQ and protect PSII from damage (Galić et al., 2020). These findings can be supported by the significant reduction in the Area value of inverted leaves at 4 p.m. (because Area refers to the free PQ pool). A positive L-band indicates a lower energy connection (Kalaji et al., 2014; Jiang et al., 2021). Both inverted and normal leaves exhibited significant positive L- and K-bands at elevated temperature and high light, but the positive L- and K-bands were more pronounced in inverted leaves than in normal leaves, indicating more severe OEC damage. Elevated temperature and high light not only affect the function of PSII but also adversely affect the electron flow on the PSI acceptor side (φ_{RO} , R_{EO}/RC , and δ_{RO}) (Kalaji et al., 2014). A large number of studies have shown that δ_{RO} values increase in plants after heat stress (Oukarroum et al., 2009; Mihaljević et al., 2020). The same, but inverted leaves exhibit higher R_{EO}/RC and δ_{RO} than normal leaves, indicating that the reduction in electron transport efficiency from the intersystem electron carrier to the PSI receptor side of the inverted leaves is even greater. High light and elevated temperature did not appear to have an effect on φ_{RO} values, as ANOVA showed no significant differences between treatments; however, inverted leaves had significantly lower φ_{RO} compared with normal leaves, which may be due to a reduction in PSI content in inverted leaves (Yan et al., 2013). In this study, F_V/F_O was significantly lower in inverted and normal leaves under high light and elevated temperature, but the decrease was higher in inverted leaves than in normal leaves, indicating that electron transport was impaired during photosynthesis in inverted leaves compared to normal leaves, which is similar to the results of Janka et al. (2020) who treated microalgae (*Tetradesmus wisconsinensis*) with bicarbonate.

The overall photosynthetic performance of both normal and inverted leaves was reduced under elevated temperature and high light complex stress conditions, which can be explained by a decrease in the performance indexes (PI_{ABS} and PI_{total}). The expression of performance index PI_{ABS} is the product of three independent characteristics: the density of active RC per PSII antenna chlorophyll (RC/ABS), the maximum quantum efficiency of PSII (F_v/F_m), and the electron transport beyond Q_A (Ψ_{EO}) (Strasser et al., 2000; Kalaji et al., 2016). In this study, the decrease in PI_{ABS} appeared to be associated with a decrease in RC/ABS and Ψ_{EO} values, as the decrease in their values is greatest at elevated temperatures and high light. The PI_{ABS} values of normal and inverted leaves decreased by 63.2%–66% and 68%–90% at 4 p.m., respectively, compared to 9 a.m. Compared with PI_{ABS} , the PI_{total} values not only reflect PSII photosynthetic electron transfer activity but also relate to changes in PSI-related processes (Kalaji et al., 2014; Jiang et al., 2021). Therefore, some researchers suggest that PI_{total} is more sensitive to abiotic stresses than PI_{ABS} . Some researchers also concluded that the sensitivity of PI_{ABS} and PI_{total} to abiotic stress varied depending on environmental factors (Mallick and Mohn, 2003; Mihaljević et al., 2020). In this study, the PI_{total} values of normal and inverted leaves decreased by 24.1%–25.9% and 5.9%–66.7%, respectively, at 4 p.m. compared to 9 a.m. This is consistent with the trend in P_N values. The decrease in PI_{total} may be related to the loss of PSII activity, leading to a reduction in the electron

transport chain and disruption of PSI function (Kalaji et al., 2014; Oukarroum et al., 2018). In this study, the PI_{ABS} values of inverted leaves appeared to be more sensitive to elevated temperature and high light compared with PI_{total} . The fact that PI_{ABS} and PI_{total} were still not restored to the levels of normal leaves after the recovery of inverted leaves may be due to the higher degree of damage suffered by inverted leaves under elevated temperature and high light, and the effective repair capacity of the photosynthetic apparatus (synthesis of new proteins to replace damaged core proteins) of inverted leaves remained lower than the photooxidative damage capacity after recovery.

CONCLUSION

Stress resistance is a very important factor for the successful production of soybean in the increasingly demanding agroecological conditions. Our data indicate that a more severe photooxidative damage occurs in inverted leaves under high light and elevated temperature conditions compared to normal leaves, as evidenced by OEC inactivation, inhibition of electron transport, and inactivation of some PSII RCs. High light and elevated temperature significantly reduced the performance indexes (PI_{ABS} and PI_{total}) of inverted leaves. The PI_{ABS} values of inverted leaves were more sensitive to elevated temperature and high light. The inhibition of electron transport and the inactivation of PSII RCs in inverted leaves under combined high light and elevated temperature stresses were responsible for the significant reduction in P_n . Due to climate change, in the future, it will be required a better understanding of interactions between soybean and their environment to achieve better adaptability and thus the productivity of future cultivars.

DATA AVAILABILITY STATEMENT

The raw data supporting the conclusions of this article will be made available by the authors, without undue reservation.

AUTHOR CONTRIBUTIONS

CW and JZ designed the research. CW, JR, QG, LZ, and CL performed the research. CW, CL, and JZ analyzed the data. CW, LZ, and JZ wrote the manuscript. All authors contributed to the article and approved the submitted version.

FUNDING

This study was supported by the National Natural Science Funds of China (Grant Nos. 32160520 and 31660367) and the Xinjiang Autonomous Region Science and Technology Program (Grant No. 2020E0218).

REFERENCES

- Adamski, J. M., Peters, J. A., Danieloski, R., and Bacarin, M. A. (2011). Excess iron-induced changes in the photosynthetic characteristics of sweet potato. *J. Plant Physiol.* 168, 2056–2062. doi: 10.1016/j.jplph.2011.06.003
- Avola, G., Cavallaro, V., Patanè, C., and Riggi, E. (2008). Gas exchange and photosynthetic water use efficiency in response to light, CO₂ concentration and temperature in *Vicia faba*. *J. Plant Physiol.* 165, 796–804. doi: 10.1016/j.jplph.2007.09.004
- Bahamonde, H. A., Gil, L., and Fernández, V. (2018). Surface properties and permeability to calcium chloride of *Fagus sylvatica* and *Quercus petraea* leaves of different canopy heights. *Front. Plant Sci.* 9:494. doi: 10.3389/fpls.2018.00494
- Blackhall, V., Orioli, G., and Colavita, M. (2020). JIP-test parameters to study apple peel photosystem II behavior under high solar radiation stress during fruit development. *Photosynthetica* 58, 314–322. doi: 10.32615/ps.2019.159
- Boguszewska-Mańkowska, D., Pieczyński, M., Wyrzykowska, A., Kalaji, H., Sieczko, L., Szwejkowska-Kulińska, Z., et al. (2018). Divergent strategies displayed by potato (*Solanum tuberosum* L.) cultivars to cope with soil drought. *J. Agron Crop Sci.* 204, 13–30. doi: 10.1111/jac.12245
- Buchner, O., Stoll, M., Karadar, M., Kranner, I., and Neuner, G. (2015). Application of heat stress in situ demonstrates a protective role of irradiation on photosynthetic performance in alpine plants. *Plant Cell Environ.* 38, 812–826. doi: 10.1111/pce.12455
- Cai, Y., Wang, L., Chen, L., Wu, T., Liu, L., Sun, S., et al. (2020). Mutagenesis of GmFT2a and GmFT5a mediated by CRISPR/Cas9 contributes for expanding the regional adaptability of soybean. *Plant Biotechnol. J.* 18, 298–309. doi: 10.1111/pbi.13199
- Ceppi, M. G., Oukarroum, A., Çiçek, N., Strasser, R. J., and Schansker, G. (2012). The IP amplitude of the fluorescence rise OJIP is sensitive to changes in the photosystem I content of leaves: a study on plants exposed to magnesium and sulfate deficiencies, drought stress and salt stress. *Physiol. Plant* 144, 277–288. doi: 10.1111/j.1399-3054.2011.01549.x
- Chen, C., Zhang, D., Li, P., and Ma, F. (2012). Partitioning of absorbed light energy differed between the sun-exposed side and the shaded side of apple fruits under high light conditions. *Plant Physiol. Biochem.* 60, 12–17. doi: 10.1016/j.plaphy.2012.07.016
- Cohen, I., Zandalinas, S. I., Fritschi, F. B., Sengupta, S., Fichman, Y., Azad, R. K., et al. (2021). The impact of water deficit and heat stress combination on the molecular response, physiology, and seed production of soybean. *Physiol. Plant* 172, 41–52. doi: 10.1111/pp.13269
- Das, R., Bhagawati, K., Boro, A., Medhi, T., Medhi, B., and Bhanisana, R. (2015). Relative performance of plant cultivars under respective water deficit adaptation strategies: a case study. *Curr. World Environ.* 10:683. doi: 10.12944/CWE.10.2.36
- Dongsansuk, A., Lütz, C., and Neuner, G. (2013). Effects of temperature and irradiance on quantum yield of PSII photochemistry and xanthophyll cycle in a tropical and a temperate species. *Photosynthetica* 51, 13–21. doi: 10.1007/s11099-012-0070-2
- Durand, M., Brendel, O., Buré, C., and Le Thiec, D. (2020). Changes in irradiance and vapour pressure deficit under drought induce distinct stomatal dynamics between glasshouse and field-grown poplars. *New Phytol.* 227, 392–406. doi: 10.1111/nph.16525
- Evans, J. R. (1999). Leaf anatomy enables more equal access to light and CO₂ between chloroplasts. *New Phytol.* 143, 93–104. doi: 10.1046/j.1469-8137.1999.00440.x
- Fanourakis, D., Hyldgaard, B., Giday, H., Aulik, I., Bouranis, D., Körner, O., et al. (2019). Stomatal anatomy and closing ability is affected by supplementary light intensity in rose (*Rosa hybrida* L.). *Hortic. Sci.* 46, 81–89. doi: 10.17221/144/2017-HORTSCI
- Faria-Silva, L., Gallon, C., Filgueiras, P., and Silva, D. (2019). Irrigation improves plant vitality in specific stages of mango tree development according to photosynthetic efficiency. *Photosynthetica* 57, 820–829. doi: 10.32615/ps.2019.091
- Farquhar, G. D., Von Caemmerer, S. V., and Berry, J. A. (1980). A biochemical model of photosynthetic CO₂ assimilation in leaves of C₃ species. *Planta* 149, 78–90. doi: 10.1007/BF00386231
- Gago, J., Douthe, C., Coopman, R. E., Gallego, P. P., Ribas-Carbo, M., Flexas, J., et al. (2015). UAVs challenge to assess water stress for sustainable agriculture. *Agric. Water Manage.* 153, 9–19. doi: 10.1016/j.agwat.2015.01.020
- Galić, V., Mazur, M., Šimić, D., Zdunić, Z., and Franić, M. (2020). Plant biomass in salt-stressed young maize plants can be modelled with photosynthetic performance. *Photosynthetica* 58, 194–204. doi: 10.32615/ps.2019.131
- Gu, J., Zhou, Z., Li, Z., Chen, Y., Wang, Z., Zhang, H., et al. (2017). Photosynthetic properties and potentials for improvement of photosynthesis in pale green leaf rice under high light conditions. *Front. Plant Sci.* 8:1082. doi: 10.3389/fpls.2017.01082
- Hazrati, S., Tahmasebi-Sarvestani, Z., Modarres-Sanavy, S. A. M., Mokhtassi-Bidgoli, A., and Nicola, S. (2016). Effects of water stress and light intensity on chlorophyll fluorescence parameters and pigments of *Aloe vera* L. *Plant Physiol. Biochem.* 106, 141–148. doi: 10.1016/j.plaphy.2016.04.046
- Hughes, N. M., and Smith, W. K. (2007). Attenuation of incident light in *Galax urceolata* (Diapensiaceae): concerted influence of adaxial and abaxial anthocyanin layers on photoprotection. *Am. J. Bot.* 94, 784–790. doi: 10.3732/ajb.94.5.784
- Hussain, S., Iqbal, N., Brestic, M., Raza, M. A., Pang, T., Langham, D. R., et al. (2019). Changes in morphology, chlorophyll fluorescence performance and Rubisco activity of soybean in response to foliar application of ionic titanium under normal light and shade environment. *Sci. Total Environ.* 658, 626–637. doi: 10.1016/j.scitotenv.2018.12.182
- IPCC (2019). “Summary for policymakers,” in *Climate Change and Land: an IPCC Special Report on Climate Change, Desertification, Land Degradation, Sustainable Land Management, Food Security, and Greenhouse Gas Fluxes in Terrestrial Ecosystems*, eds P. R. Shukla, J. Skea, E. Calvo Buendia, V. Masson-Delmotte, H.-O. Portner, D. C. Roberts, et al. (Geneva: Intergovernmental Panel on Climate Change). doi: 10.1002/9781118786352.wbieg0538
- Janka, E., Körner, O., Rosenqvist, E., and Ottosen, C.-O. (2013). High temperature stress monitoring and detection using chlorophyll a fluorescence and infrared thermography in chrysanthemum (*Dendranthema grandiflora*). *Plant Physiol. Biochem.* 67, 87–94. doi: 10.1016/j.plaphy.2013.02.025
- Janka, E., Umetani, I., Sposob, M., and Bakke, R. (2020). Photosynthesis response of microalgae (*Tetrademus wisconsinensis*) to different inorganic carbon sources probed with chlorophyll fluorescence analysis. *Photosynthetica* 58, 236–244. doi: 10.32615/ps.2019.142
- Jiang, H., Chen, L., Zheng, J., Han, S., Tang, N., and Smith, B. (2008). Aluminum-induced effects on Photosystem II photochemistry in *Citrus* leaves assessed by the chlorophyll a fluorescence transient. *Tree Physiol.* 28, 1863–1871. doi: 10.1093/treephys/28.12.1863
- Jiang, Y., Feng, X., Wang, H., Chen, Y., and Sun, Y. (2021). Heat-induced down-regulation of photosystem II protects photosystem I in honeysuckle (*Lonicera japonica*). *J. Plant Res.* 134, 1311–1321. doi: 10.1007/s10265-021-01336-x
- Kalaji, H. M., Carpentier, R., Allakhverdiev, S. I., and Bosa, K. (2012). Fluorescence parameters as early indicators of light stress in barley. *J. Photochem. Photobiol. B Biol.* 112, 1–6. doi: 10.1016/j.jphotobiol.2012.03.009
- Kalaji, H. M., Jajoo, A., Oukarroum, A., Brestic, M., Zivcak, M., Samborska, I. A., et al. (2016). Chlorophyll a fluorescence as a tool to monitor physiological status of plants under abiotic stress conditions. *Acta Physiol. Plant* 38:102. doi: 10.1007/s11738-016-2113-y
- Kalaji, H. M., Oukarroum, A., Alexandrov, V., Kouzmanova, M., Brestic, M., Zivcak, M., et al. (2014). Identification of nutrient deficiency in maize and tomato plants by *in vivo* chlorophyll a fluorescence measurements. *Plant Physiol. Biochem.* 81, 16–25. doi: 10.1016/j.plaphy.2014.03.029
- Kimm, H., Guan, K., Burroughs, C. H., Peng, B., Ainsworth, E. A., Bernacchi, C. J., et al. (2021). Quantifying high-temperature stress on soybean canopy photosynthesis: the unique role of sun-induced chlorophyll fluorescence. *Glob. Change Biol.* 27, 2403–2415. doi: 10.1111/gcb.15603
- Krause, G., and Weis, E. (1991). Chlorophyll fluorescence and photosynthesis: the basics. *Annu. Rev. Plant Biol.* 42, 313–349. doi: 10.1146/annurev.pp.42.060191.001525
- Krieger-Liszka, A., Fufezan, C., and Trebst, A. (2008). Singlet oxygen production in photosystem II and related protection mechanism. *Photosynthesis Res.* 98, 551–564. doi: 10.1007/s11120-008-9349-3
- Li, P. D., Zhu, Y. F., Song, X. L., and Song, F. P. (2020). Negative effects of long-term moderate salinity and short-term drought stress on the photosynthetic

- performance of Hybrid *Pennisetum*. *Plant Physiol. Biochem.* 155, 93–104. doi: 10.1016/j.plaphy.2020.06.033
- Mallik, N., and Mohn, F. (2003). Use of chlorophyll fluorescence in metal-stress research: a case study with the green microalga *Scenedesmus*. *Ecotoxicol. Environ. Saf.* 55, 64–69. doi: 10.1016/S0147-6513(02)00122-7
- Marcinińska, I., Czaczyło-Mysza, I., Skrzypek, E., Grzesiak, M. T., Popielarska-Konieczna, M., Warchoł, M., et al. (2017). Application of photochemical parameters and several indices based on phenotypical traits to assess intraspecific variation of oat (*Avena sativa* L.) tolerance to drought. *Acta Physiol. Plant* 39, 1–13. doi: 10.1007/s11738-017-2453-2
- Mihaljević, I., Lepeduš, H., Šimić, D., Vuletić, M. V., Tomaš, V., Vuković, D., et al. (2020). Photochemical efficiency of photosystem II in two apple cultivars affected by elevated temperature and excess light *in vivo*. *S. Afr. J. Bot.* 130, 316–326. doi: 10.1016/j.sajb.2020.01.017
- Oukarroum, A., Lebrihi, A., El Gharous, M., Goltsev, V., and Strasser, R. J. (2018). Desiccation-induced changes of photosynthetic transport in *Parmelina tiliacea* (Hoffm.) Ach. analysed by simultaneous measurements of the kinetics of prompt fluorescence, delayed fluorescence and modulated 820 nm reflection. *J. Lumin.* 198, 302–308. doi: 10.1016/j.jlumin.2018.02.040
- Oukarroum, A., Schansker, G., and Strasser, R. J. (2009). Drought stress effects on photosystem I content and photosystem II thermotolerance analyzed using Chl a fluorescence kinetics in barley varieties differing in their drought tolerance. *Physiol. Plant* 137, 188–199. doi: 10.1111/j.1399-3054.2009.01273.x
- Pandey, R., Chacko, P. M., Choudhary, M., Prasad, K., and Pal, M. (2007). Higher than optimum temperature under CO₂ enrichment influences stomata anatomical characters in rose (*Rosa hybrida*). *Sci. Hortic. Amsterdam* 113, 74–81. doi: 10.1016/j.scienta.2007.01.021
- Paradiso, R., De Visser, P. H., Arena, C., and Marcelis, L. F. (2020). Light response of photosynthesis and stomatal conductance of rose leaves in the canopy profile: the effect of lighting on the adaxial and the abaxial sides. *Funct. Plant Biol.* 47, 639–650. doi: 10.1071/FP19352
- Proietti, P., and Palliotti, A. (1997). Contribution of the adaxial and abaxial surfaces of olive leaves to photosynthesis. *Photosynthetica* 33, 63–69. doi: 10.1023/A:1022175221813
- Rastogi, A., Kovar, M., He, X., Zivcak, M., Kataria, S., Kalaji, H., et al. (2020). JIP-test as a tool to identify salinity tolerance in sweet sorghum genotypes. *Photosynthetica* 58, 518–528. doi: 10.32615/ps.2019.169
- Schansker, G., Tóth, S. Z., and Strasser, R. J. (2005). Methylviologen and dibromothymoquinone treatments of pea leaves reveal the role of photosystem I in the Chl a fluorescence rise OJIP. *BBA Bioenergetics* 1706, 250–261. doi: 10.1016/j.bbabi.2004.11.006
- Stefanov, D., Petkova, V., and Denev, I. D. (2011). Screening for heat tolerance in common bean (*Phaseolus vulgaris* L.) lines and cultivars using JIP-test. *Sci. Hortic. Amsterdam* 128, 1–6. doi: 10.1016/j.scienta.2010.12.003
- Strasser, R. J., and Srivastava, A. (1995). Polyphasic chlorophyll a fluorescence transient in plants and cyanobacteria. *Photochem. Photobiol.* 61, 32–42. doi: 10.1111/j.1751-1097.1995.tb09240.x
- Strasser, R. J., Srivastava, M., and Tsimilli-Michael, M. (2000). “The fluorescence transient as a tool to characterize and screen photosynthetic samples,” in *Probing Photosynthesis: Mechanisms, Regulation and Adaption*, eds M. Yunus, U. Pathre, and P. Mohanty (London: Taylor & Francis).
- Strasser, R. J., Tsimilli-Michael, M., and Srivastava, A. (2004). “Analysis of the fluorescence transient,” in *Chlorophyll Fluorescence: a Signature of Photosynthesis*, eds G. C. Papageorgiou and Govindjee (Dordrecht: Springer), 321–367.
- Strasser, R. J., Tsimilli-Michael, M., Qiang, S., and Goltsev, V. (2010). Simultaneous *in vivo* recording of prompt and delayed fluorescence and 820-nm reflection changes during drying and after rehydration of the resurrection plant *Haberlea rhodopensis*. *BBA Bioenergetics* 1797, 1313–1326. doi: 10.1016/j.bbabi.2010.03.008
- Tóth, S. Z., Schansker, G., and Strasser, R. J. (2007). A non-invasive assay of the plastoquinone pool redox state based on the OJIP-transient. *Photosynthesis Res.* 93, 193–203. doi: 10.1007/s11120-007-9179-8
- Uhrmacher, S., Hanelt, D., and Nultsch, W. (1995). Zeaxanthin content and the degree of photoinhibition are linearly correlated in the brown alga *Dictyota dichotoma*. *Mar. Biol.* 123, 159–165. doi: 10.1007/BF00350335
- Xu, W., Deng, X., and Xu, B. (2013). Effects of water stress and fertilization on leaf gas exchange and photosynthetic light-response curves of *Bothriochloa ischaemum* L. *Photosynthetica* 51, 603–612. doi: 10.1007/s11099-013-0061-y
- Yamori, W., and Shikanai, T. (2016). Physiological functions of cyclic electron transport around photosystem I in sustaining photosynthesis and plant growth. *Annu. Rev. Plant Biol.* 67, 81–106. doi: 10.1146/annurev-arplant-043015-112002
- Yan, K., Chen, P., Shao, H., Shao, C., Zhao, S., and Brestic, M. (2013). Dissection of photosynthetic electron transport process in sweet sorghum under heat stress. *PLoS One* 8:e62100. doi: 10.1371/journal.pone.0062100
- Zhang, Z.-S., Li, Y.-T., Gao, H.-Y., Yang, C., and Meng, Q.-W. (2016). Characterization of photosynthetic gas exchange in leaves under simulated adaxial and abaxial surfaces alternant irradiation. *Sci. Rep.* 6, 1–11. doi: 10.1038/srep26963

Conflict of Interest: The authors declare that the research was conducted in the absence of any commercial or financial relationships that could be construed as a potential conflict of interest.

Publisher's Note: All claims expressed in this article are solely those of the authors and do not necessarily represent those of their affiliated organizations, or those of the publisher, the editors and the reviewers. Any product that may be evaluated in this article, or claim that may be made by its manufacturer, is not guaranteed or endorsed by the publisher.

Copyright © 2022 Wang, Gu, Zhao, Li, Ren and Zhang. This is an open-access article distributed under the terms of the Creative Commons Attribution License (CC BY). The use, distribution or reproduction in other forums is permitted, provided the original author(s) and the copyright owner(s) are credited and that the original publication in this journal is cited, in accordance with accepted academic practice. No use, distribution or reproduction is permitted which does not comply with these terms.